

## Experimental simulations of CH<sub>4</sub> evaporation on Titan

A. Luspay-Kuti,<sup>1</sup> V. F. Chevrier,<sup>1</sup> F. C. Wasiak,<sup>1</sup> L. A. Roe,<sup>1</sup> W. D. D. P. Welivitiya,<sup>1</sup>  
T. Cornet,<sup>2</sup> S. Singh,<sup>1</sup> and E. G. Rivera-Valentin<sup>3</sup>

Received 25 September 2012; revised 1 November 2012; accepted 5 November 2012; published 14 December 2012.

[1] We present the first experimental results on the evaporation of liquid CH<sub>4</sub> under simulated Titan surface conditions similar to those observed at the Huygens landing site. An average evaporation rate of  $(3.1 \pm 0.6) \times 10^{-4}$  kg s<sup>-1</sup> m<sup>-2</sup> at 94 K and 1.5 bar was measured. While our results are generally higher than previous models based on energy balance, they show an excellent match with a theoretical mass transfer approach. Indeed, we find that evaporation in the Titan environmental chamber is predominantly diffusion driven and affected by the buoyancy of lighter CH<sub>4</sub> in the heavier N<sub>2</sub> atmosphere. After correcting for the difference in gravity of Earth and Titan, the resulting evaporation rate is  $(1.6 \pm 0.3) \times 10^{-4}$  kg s<sup>-1</sup> m<sup>-2</sup> (or  $1.13 \pm 0.3$  mm hr<sup>-1</sup>). Using our experimental evaporation rates, we determine that the low-latitude storm recently observed by Cassini ISS would have resulted in a maximum evaporated mass of  $(5.4 \pm 1.2) \times 10^{10}$  kg of CH<sub>4</sub> equivalent to a  $2.4 \pm 0.5$  m thick layer over 80 days. Based on our results, a sufficient amount of CH<sub>4</sub> can accumulate in the otherwise arid equatorial regions to produce transient ponds and liquid flows. **Citation:** Luspay-Kuti, A., V. F. Chevrier, F. C. Wasiak, L. A. Roe, W. D. D. P. Welivitiya, T. Cornet, S. Singh, and E. G. Rivera-Valentin (2012), Experimental simulations of CH<sub>4</sub> evaporation on Titan, *Geophys. Res. Lett.*, 39, L23203, doi:10.1029/2012GL054003.

### 1. Introduction

[2] Liquids have been suggested to be stable on the surface of Titan well before the arrival of the Cassini-Huygens mission. The fact that surface conditions are near the triple point of methane and ethane, and the detection of CH<sub>4</sub> in Titan's atmosphere [Kuiper, 1944; Lunine et al., 1983] led to the conclusion that large bodies of liquids, and possibly oceans, may exist. Though we now know there are no surface oceans, various evidence from the Cassini-Huygens mission demonstrated the unambiguous presence of liquid lakes and seas on the surface [Stofan et al., 2007]. These bodies of liquid seem to be confined to the colder and supposedly more humid polar regions, while at low latitudes vast longitudinal dunes are pervasive [Lorenz and Radebaugh, 2009]. Although the dunes indicate dry, desert-like condi-

tions [Lorenz et al., 2006], the presence of dendritic channels [Lorenz et al., 2008], observed cobbles [Tomasko et al., 2005] and subsurface CH<sub>4</sub> moisture detected by the GCMS at the Huygens landing site [Niemann et al., 2005, 2010] show evidence for liquid in some form and amount at low latitudes at some point in Titan's history.

[3] Recently, Cassini's Imaging Science Subsystem (ISS) detected a large low latitude storm system accompanied by extensive surface changes [Turtle et al., 2011], suggesting that the observed surface darkening during the storm and the fluvial features intersecting the dune fields may form as a result of occasional heavy rainfall events. Since CH<sub>4</sub> is thought to be the primary component of Titan's hydrological cycle, precipitation at low latitudes would predominantly be composed methane. Furthermore, Griffith et al. [2012] report on possible tropical lakes from Cassini VIMS near-infrared spectra.

[4] Thermal models and GCMs [Mitchell, 2008; Schneider et al., 2012] require evaporation/precipitation rates for simulating the hydrological cycle and surface-atmosphere interactions all over the satellite. The use of approximated evaporation values from energy balance or parameters adapted to fit observations requires validation by experiments that were lacking until now. Therefore, we developed a Titan simulation chamber to address this deficiency in the literature and we present the first experimental measurements on the evaporation rate of liquid CH<sub>4</sub> under simulated Titan conditions similar to those observed at the Huygens landing site. We discuss the implications of our results on the stability of low latitude liquids on the surface of Titan.

### 2. Experiment

[5] The experimental facility is specifically designed to simulate the surface environment of Titan (auxiliary material).<sup>1</sup> Temperatures of 90–95 K are reproduced via liquid nitrogen, while a 1.5 bar atmosphere is maintained with pressurized N<sub>2</sub>. Once the required temperatures and pressures are achieved, we introduce CH<sub>4</sub> into a condenser inside the Titan module then drain the liquid methane into a 15 cm diameter pan. Mass loss of liquid CH<sub>4</sub> over time, along with temperatures at various locations (Figure S1 in the auxiliary material) within the Titan module, are continuously recorded. A gas chromatograph equipped with a flame ionization detector is used to measure CH<sub>4</sub> concentration inside the chamber, from which the CH<sub>4</sub> partial pressure and mole fraction characterizing our runs are calculated. Based on these measurements, we maintain a CH<sub>4</sub> mole fraction of  $\sim 2 \times 10^{-2}$ , which is slightly lower than  $4.92 \times 10^{-2}$ , as measured at the Huygens landing

<sup>1</sup>Arkansas Center for Space and Planetary Sciences, University of Arkansas, Fayetteville, Arkansas, USA.

<sup>2</sup>Laboratoire de Planétologie et Géodynamique de Nantes, UMR 6112, CNRS, OSUNA, Nantes, France.

<sup>3</sup>Department of Geological Sciences, Brown University, Providence, Rhode Island, USA.

Corresponding author: A. Luspay-Kuti, Arkansas Center for Space and Planetary Sciences, University of Arkansas, FELD 202, Fayetteville, AR 72701, USA. (aluspayk@uark.edu)

<sup>1</sup>Auxiliary materials are available in the HTML. doi:10.1029/2012GL054003.

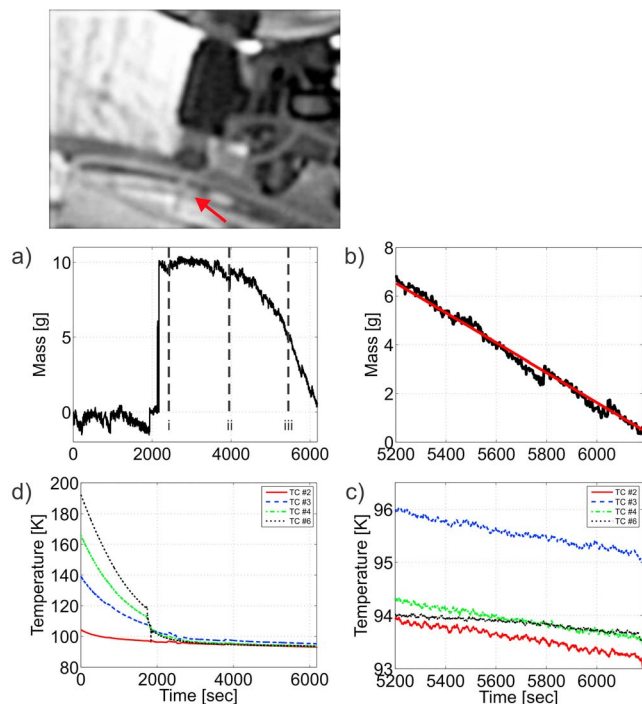


**Figure 1.** Example run of an evaporation experiment. (top left) Captured image of liquid CH<sub>4</sub> (indicated by arrow) pouring out of the condenser through the solenoid valve. The edge of the sample pan is seen near the bottom of the image. (a) Mass as a function of time throughout the entire run. The vertical dashed lines indicate the distinguished phases of the experiment (sections i - iii). Between sections i and ii there is a plateau caused by ongoing heat transfer between the colder liquid and the warmer ambient atmosphere. The plateau is followed by a section of non-steady state evaporation as the liquid and atmosphere equilibrate (section iii). (b) Steady-state evaporation; magnified section of iii in Figure 1a). The slope of this curve determines the evaporation rate. The linear fit is marked by the red line. (d, c) Corresponding temperatures.

site [Niemann *et al.*, 2005]. For a detailed description on the chamber see Wasiak *et al.* [2012].

### 3. Results

#### 3.1. Mass Profile

[6] The mass data presented in Figure 1a can be divided into three distinctive parts. Under the extreme conditions inside the chamber, small changes in pressure and temperature often induce fluctuations relative to an electronic zero (tare), which is the reason for occasional negative mass before condensation (Figure 1a, section i). At the end of part i, the sudden jump in mass (at around 2100 sec in Figure 1) occurs when liquid CH<sub>4</sub> is poured into the pan after condensation. In this specific case, ~10 g of CH<sub>4</sub> was condensed. That section is followed by an apparent plateau (Figure 1a, section i-ii), where the mass stays approximately constant over ~1800 seconds. This is caused by ongoing heat transfer between the colder liquid and the warmer surrounding gas at the time of introduction of condensed CH<sub>4</sub> into the system. Based on later CH<sub>4</sub>-C<sub>2</sub>H<sub>6</sub> mixture runs that are not

discussed here and considering the reproducibility of our experiments, the condensed CH<sub>4</sub> has a temperature of 92 K, while the surrounding atmosphere is still relatively warm, with a temperature of ~100 K over the time of the plateau. Using the heat transfer coefficient of the process and the density and specific heat of liquid CH<sub>4</sub>, an estimate for the thermal time constant can be provided. The heat transfer coefficient is determined from the ratio of the characteristic length and the heat conductivity of N<sub>2</sub>. According to first-order calculations using the lumped capacitance method (see auxiliary material), the time required for the liquid to reach a temperature of 94 K is ~1780 seconds, which is comparable to the observed time-span of the plateau.

[7] After the plateau, the data shows a slightly decreasing trend, which indicates increased non-steady state evaporation as the liquid sufficiently warms. This is then followed by a linear portion, which corresponds to the start of steady state evaporation (Figure 1b). By that time, the ambient chamber temperature cools down to 94 K.

#### 3.2. Methane Evaporation

[8] Evaporation rates are calculated by first finding the linear portion in the mass vs. time curves (Figure 1b) where the atmospheric temperature in the chamber remains below 95 K. A least-squares fit to the data is performed in order to determine the evaporation rate for a given temperature range as the slope of the regression line with corresponding uncertainties to a 95% confidence interval. Based on four separate runs with the same experimental setup and similar simulated conditions, we determined an evaporation rate of  $(3.1 \pm 0.6) \times 10^{-4} \text{ kg s}^{-1} \text{ m}^{-2}$ .

### 4. Discussion

#### 4.1. Evaporation Theory and Effect of Buoyancy

[9] Since methane is lighter than molecular N<sub>2</sub>, buoyancy is expected to affect evaporation. This appears to be the case for both our experimental setup and the atmosphere of Titan where the average weight is 28 g mol<sup>-1</sup> compared to CH<sub>4</sub>'s 16 g mol<sup>-1</sup>. Buoyancy-driven evaporation is estimated by a modified mass flux equation originally developed for martian ice [Ingersoll, 1970]:

$$J = 0.17 D_{CH_4/N_2} \Delta \eta \left( \frac{\Delta \rho g}{\rho_{surf} \nu^2} \right)^{\frac{1}{3}}, \quad (1)$$

where  $D_{CH_4/N_2}$  is the diffusion coefficient of CH<sub>4</sub> gas in N<sub>2</sub> [Elliott and Watts, 1972],  $\Delta \eta = \rho_{surf}^{CH_4, gas} - \rho_{atm}^{CH_4, gas}$  is the difference between the density of CH<sub>4</sub> above the liquid layer and the density of CH<sub>4</sub> in the ambient atmosphere,  $\Delta \rho = \rho_{atm} - \rho_{surf}$  is the difference between the density of the ambient gas and the gas at the surface,  $g$  is the gravitational acceleration on Titan, and  $\nu$  is the kinematic viscosity of CH<sub>4</sub> [Crane Co., 1982]. These parameters and their values are summarized in Table 1 (for additional information on the used parameters, see auxiliary material). Buoyancy-driven evaporation rates on Earth are expected to be larger relative to those in Titan's gravity field with a factor of  $E_{Titan}/E_{Earth} = (g_{Titan}/g_{Earth})^{1/3} = 0.516$ . Thus, the average evaporation rate from our simulations, corrected for the gravity field of Titan is  $(1.6 \pm 0.3) \times 10^{-4} \text{ kgs}^{-1} \text{ m}^{-2}$ .

**Table 1.** Measured and Calculated Parameters in methane Evaporation Experiments<sup>a</sup>

Evaporation Rate (kg m <sup>-2</sup> s <sup>-1</sup> )	Average Temperature (K)	Pressure (bar)	CH <sub>4</sub> Mole Fraction
$(2.2 \pm 0.02) \times 10^{-4}$	94.0	1.5	N/A
$(3.4 \pm 0.01) \times 10^{-4}$	95.0	1.5	$2.3 \times 10^{-2}$
$(3.3 \pm 0.01) \times 10^{-4}$	93.7	1.5	$1.9 \times 10^{-2}$
$(3.2 \pm 0.02) \times 10^{-4}$	93.7	1.5	$2.2 \times 10^{-2}$
$\langle E_{\text{exp}} \rangle = (3.1 \pm 0.6) \times 10^{-4}$	$94.1 \pm 0.6$	1.5	$2.1 \times 10^{-2}$
$\langle E_{\text{corr}} \rangle = (1.6 \pm 0.3) \times 10^{-4}$	<b><math>94.1 \pm 0.6</math></b>	<b>1.5</b>	<b><math>2.1 \times 10^{-2}</math></b>

<sup>a</sup> $\langle E_{\text{exp}} \rangle$  is the averaged evaporation data measured in the experiments, and  $\langle E_{\text{corr}} \rangle$  is the average evaporation rate corrected for the difference between Earth's and Titan's gravity.

## 4.2. Liquid Composition

[10] Considering the solubility of N<sub>2</sub> in CH<sub>4</sub>, we suggest a binary mixture of CH<sub>4</sub>-N<sub>2</sub> for the composition of the evaporating liquid in the chamber. Assuming N<sub>2</sub> is only mixed when the CH<sub>4</sub> is in contact with the chamber atmosphere, the time it takes for the mixture to equilibrate is only 10 seconds. This is due to the high diffusion coefficient of N<sub>2</sub> into liquid CH<sub>4</sub>. We calculate that the mole fractions of N<sub>2</sub> and CH<sub>4</sub> in the condensed liquid is 0.16 and 0.84 respectively (see auxiliary material). Using Ingersoll's equation (equation (1)) and dividing it by the density of the binary mixture (Table 2), we derive an evaporation rate of  $1.52 \times 10^{-4}$  kgs<sup>-1</sup>m<sup>-2</sup>. This value is in excellent agreement with the gravity-corrected experimental value of  $(1.58 \pm 0.3) \times 10^{-4}$  kg s<sup>-1</sup>m<sup>-2</sup>.

[11] To examine the possibility of a pure CH<sub>4</sub> liquid evaporating in the chamber, we performed the same calculations from equation (1) for a CH<sub>4</sub> mole fraction of 1. The resulting evaporation rate of  $2.31 \times 10^{-4}$  kgs<sup>-1</sup>m<sup>-2</sup> largely overestimates the experimentally measured rate, with an error of 31.5%.

[12] We conclude that based on the good agreement of the experimentally determined and gravity corrected evaporation rate and the theoretical approach, the composition of the evaporating liquid in the chamber is a CH<sub>4</sub>-N<sub>2</sub> binary mixture with mole fractions of 0.84 and 0.16 respectively. The fact that Ingersoll's equation predicts the evaporation rate in the chamber demonstrates that mass transfer in our experiments is largely controlled by the concentration difference in the simulated atmosphere and buoyancy-driven diffusion.

## 4.3. Implications for Titan

[13] Although lakes are not observed at the low latitude regions of Titan, transient liquids may still exist for limited periods of time [Griffith *et al.*, 2012]. Recent observations of a low-latitude storm and accompanied surface darkening may indicate temporal liquid CH<sub>4</sub> accumulation [Turtle *et al.*, 2011]. Assuming the reported surface changes are in fact due to CH<sub>4</sub> precipitation and possibly standing liquid on the surface, rough quantitative estimates on the depth of evaporated CH<sub>4</sub> and the total mass of precipitation can be made based on the experimental evaporation rates presented here. The storm onset was reported to be around 27 September 2010, accompanying surface changes were observed through October 2010, and most changes reverted by 15 January 2011 [Turtle *et al.*, 2011]. The area subject to albedo changes seen by ISS until 29 October 2010 was  $510,000 \pm 20,000$  km<sup>2</sup> [Turtle *et al.*, 2011]. Assuming that all the CH<sub>4</sub>

precipitated between the onset and 29 October 2010, in order for the darkened terrain to reverse to normal, all the accumulated CH<sub>4</sub> had to evaporate by 15 January 2011.

[14] Using our experimentally determined evaporation rate and the time between 29 October, 2010 and 15 January 2011, the maximum depth of the evaporated liquid resulting from the storm is  $2.4 \pm 0.5$  m. Once multiplied by the area of observed changes ( $510,000$  km<sup>2</sup>) and the density of the CH<sub>4</sub>-N<sub>2</sub> mixture at 94 K, this corresponds to a maximum total mass of  $(5.4 \pm 1.2) \times 10^{10}$  kg of evaporated/precipitated CH<sub>4</sub>.

[15] It is important to note that our mass and depth estimates are an upper limit, because the evaporation of the CH<sub>4</sub>-N<sub>2</sub> mixture is predominantly diffusion-driven in our experiments, while numerical models and GCMs predict heat balance driven evaporation [Schneider *et al.*, 2012; Williams *et al.*, 2012; Mitchell, 2008]. Indeed, energy transfer is limited on Titan as shown by McKay *et al.* [1991] and more recently by Williams *et al.* [2012], and thus leads to significantly lower evaporation rates. Alternatively, our results indicate that the main driver for CH<sub>4</sub> evaporation under Titan conditions is buoyancy-driven, although an energy source is still required for the phase change to occur. Considering the extremely low temperatures during our experiments, radiation from the chamber walls is negligible; however, additional energy sources could arise from the cooling of the liquid during diffusion and heat conduction from the bottom of the liquid to the colder top layer. A detailed heat transfer study will be presented in a future paper, nonetheless the results of our experiments suggest that even in an energy-limited environment, the evaporation process can still be controlled by mass transfer.

[16] On Titan, according to the model of Williams *et al.* [2012], the daily average non-radiative fluxes are 20 times higher than previously thought [McKay *et al.*, 1991], and are theoretically available for convective energy. At the same time, we do not see any evidence for active convection in the chamber, only for passive convection in the form of buoyancy. Indeed, as shown in Figures 1d and 1c, the temperature close to the pan remains cooler than in the ambient atmosphere of the chamber during both the steady-state and the plateau periods. Moreover, the temperature profiles remain very parallel and show an overall decreasing trend (Figure 1c). These observations are indicative of heat conduction from the warmer upper gas downward into the

**Table 2.** Parameters and Their Values Used in Equation (1) for a CH<sub>4</sub>-N<sub>2</sub> Liquid

Parameter	Symbol	Value
Surface temperature	T	94 K
Surface pressure	P <sub>tot</sub>	1.5 bar
Saturation density of CH <sub>4</sub> vapor	$\rho_{\text{surf}}^{\text{CH}_4, \text{gas}}$	$0.37 \text{ kg m}^{-3}$
Initial atmospheric CH <sub>4</sub> density	$\rho_{\text{atm}}^{\text{CH}_4, \text{gas}}$	$0.15 \text{ kg m}^{-3}$
Liquid density	$\rho_{\text{liq}}$	$501.32 \text{ kg m}^{-3}$
Mole fraction of CH <sub>4</sub> in liquid	X <sub>CH<sub>4</sub></sub>	0.84
Density of liquid CH <sub>4</sub>	$\rho_{\text{CH}_4}$	$442.8 \text{ kg m}^{-3}$
Density of N <sub>2</sub>	$\rho_{\text{N}_2}$	$808.6 \text{ kg m}^{-3}$
Molecular mass of CH <sub>4</sub>	M <sub>CH<sub>4</sub></sub>	$0.016 \text{ kg mol}^{-1}$
Saturation mole fraction of CH <sub>4</sub>	Y <sub>CH<sub>4</sub></sub>	0.119
Diffusion coefficient	D <sub>CH<sub>4</sub>/N<sub>2</sub></sub>	$1.89 \times 10^{-6} \text{ m}^2 \text{ s}^{-1}$
Density of ambient gas	$\rho_{\text{atm}}$	5.26
Density of gas at the surface	$\rho_{\text{surf}}$	5.09
Gravitational acceleration	g	$1.35 \text{ m s}^{-2}$
Kinematic viscosity	$\nu$	$1.16 \times 10^{-6} \text{ m}^2 \text{ s}^{-1}$

liquid. The biggest temperature difference occurs between the uppermost and lowermost positioned thermocouples (TC #3 and TC #2 in Figure S1). Considering that the error for the K type thermocouples used is about 1°C, the thermocouples may hint at a statistically significant thermal gradient between these two thermocouples, though, if so, the gradient is very small. For the other thermocouples, the uncertainties resulting from the temperature readings makes these temperature gradients statistically not unique. By the onset of the steady-state section, where the evaporation rates were determined, sufficient time has elapsed such that the system reaches similar temperatures within error (standard deviations of 0.75, 0.96, 0.48 and 0.18 K for thermocouple #s 2, 3, 4 and 6, respectively).

[17] Additionally, since the exact onset and offset of precipitation over the course of the low latitude storm is unknown, we may be overestimating the depth and mass. The differences in topography will cause a non-uniform distribution of liquid due to runoff with deeper and shallower areas. Processes other than evaporation, such as infiltration are important as well (as indicated by the presence of subsurface CH<sub>4</sub> moisture detected by the Huygens GCMS [Niemann *et al.*, 2005]), but are not within the scope of the present work.

#### 4.4. Effect of Wind

[18] Wind speeds at the surface of Titan are generally weak with speeds of 0.2–1 m s<sup>-1</sup> [Lorenz, 2006]. Based on the model of Mitri *et al.* [2007], evaporation, or rather the flux, is linearly proportional to wind speed. To examine the maximum effect of wind, we assume the highest wind speeds of 1 m s<sup>-1</sup> and calculate the mass flux from the equation of Mitri *et al.* [2007]  $E = \rho_{\text{am}} K (q^* - q) u_r$ , where  $K$  is the transfer coefficient (0.0013 [Mitri *et al.*, 2007]),  $q^*$  and  $q$  are the saturation specific humidity and specific humidity of CH<sub>4</sub>, respectively, and  $u_r$  is the horizontal wind speed. Dividing by the density of the binary mixture we get a value of 1.65 mm hr<sup>-1</sup>. The corrected evaporation rate in our experiments - as mentioned before - is 1.13 ± 0.3 mm hr<sup>-1</sup>. Since wind removes humidity over the liquid, we are taking the effect of wind into consideration by assuming a dry N<sub>2</sub> atmosphere in our calculations. Considering the excellent agreement of our experimental results with Ingersoll's equation (equation (1)), we used that in our calculations. Assuming a dry Titanian atmosphere of 1.5 bar of N<sub>2</sub>, the evaporation rate of the mixture would be 2.6 mm hr<sup>-1</sup>, almost 2.5 times faster than in a humid atmosphere. That would result in an evaporated liquid of 1.2 × 10<sup>11</sup> kg over the low latitude storm reported by Turtle *et al.* [2011] under windy Titan conditions. This again is an upper bound, considering the overestimation of the mass and depth of evaporated liquid from our evaporation rates and a completely dry atmosphere.

#### 5. Conclusions

[19] Based on our results evaporation is predominantly diffusion-driven in the chamber, although we cannot exclude possible minor additional energy sources that could contribute to the evaporation. Whatever the driver process (energy or mass), the resulting fluxes (from mass or heat transfer) should converge to the same value. We find that the composition of our samples is most adequately a binary

mixture of CH<sub>4</sub> with dissolved N<sub>2</sub> with mole fractions of 84% and 16% respectively. We provide an upper limit of 1.13 ± 0.3 mm hr<sup>-1</sup> for the evaporation rate of such a binary mixture, driven by the concentration difference and buoyancy in the chamber. Assuming that as the main evaporation process on the surface of Titan, we propose a maximum depth of 2.4 ± 0.5 m and a maximum evaporated mass of (5.4 ± 1.2) × 10<sup>10</sup> kg during the low-latitude storm seen by Cassini ISS, reported by Turtle *et al.* [2011]. Considering the significance of diffusion and buoyancy in our experiments and the effect of heat balance in the models, we propose that evaporation on Titan is most probably a combination of these effects, and so, should be taken into account in modeling. At the same time, the results of our experiments provide an upper bound to the evaporation of liquid CH<sub>4</sub> on Titan. Our results are within the model estimates of 0.5–15 mm hr<sup>-1</sup>, thought to be required for the formation of fluvial features [Perron *et al.*, 2006]. This implies that ponding, and even liquid flow may be possible depending on the local topography, explaining the observed fluvial features at the arid low latitudes. If diffusion and buoyancy are nearly as important on Titan as in our simulation chamber, this binary mixture will evaporate significantly faster than ternary liquids for purely energy controlled models, in agreement with the presence of dunes at the same time, in spite of the occasional heavy storm events.

[20] **Acknowledgments.** This work was funded by NASA OPR NNX10AE10G. The authors would like to thank Chris McKay and Mathieu Choukroun for improving the paper with their comments.

[21] The Editor thanks Mathieu Choukroun and an anonymous reviewer for their assistance in evaluating this paper.

#### References

- Crane Co. (1982), Flow of fluids through valves, fittings and pipe, *Tech. Pap. 410M*, Eng. Div., New York.
- Elliott, R. W., and H. Watts (1972), Diffusion of some hydrocarbons in air: A regularity in the diffusion coefficients of a homologous series, *Can. J. Chem.*, *50*, 31–34.
- Griffith, C. A., J. M. Lora, J. Turner, P. F. Pentead, R. H. Brown, M. G. Tomasko, L. Doose, and C. See (2012), Possible tropical lakes on Titan from observations of dark terrain, *Nature*, *486*, 237–239.
- Ingersoll, A. P. (1970), Mars: Occurrence of liquid water, *Science*, *168*, 972–973.
- Kuiper, G. P. (1944), Titan: A satellite with an atmosphere, *Astrophys. J.*, *100*, 378.
- Lorenz, R. D. (2006), Thermal interactions of the Huygens probe with the Titan environment: Constraint on near-surface wind, *Icarus*, *182*, 559–566.
- Lorenz, R. D., and J. Radebaugh (2009), Global pattern of Titan's dunes: Radar survey from the Cassini prime mission, *Geophys. Res. Lett.*, *36*, L03202, doi:10.1029/2008GL036850.
- Lorenz, R. D., et al. (2006), The sand seas of Titan: Cassini RADAR observations of longitudinal dunes, *Science*, *312*, 724–727.
- Lorenz, R. D., et al. (2008), Fluvial channels on Titan: Initial Cassini RADAR observations, *Planet. Space Sci.*, *56*, 1132–1144.
- Lunine, J. I., D. J. Stevenson, and Y. L. Yung (1983), Ethane ocean on Titan, *Science*, *222*, 1229–1230.
- McKay, C. P., J. B. Pollack, and R. Courtin (1991), The greenhouse and antighouse effects on Titan, *Science*, *253*, 1118–1121.
- Mitchell, J. L. (2008), The drying of Titan's dunes: Titan's methane hydrology and its impact on atmospheric circulation, *J. Geophys. Res.*, *113*, E08015, doi:10.1029/2007JE003017.
- Mitri, G., A. P. Showman, J. I. Lunine, and R. D. Lorenz (2007), Hydrocarbon lakes on Titan, *Icarus*, *186*, 385–394.
- Niemann, H. B., et al. (2005), The abundances of constituents of Titan's atmosphere from the GCMS instrument on the Huygens probe, *Nature*, *438*, 779–784.
- Niemann, H. B., S. K. Atreya, J. E. Demick, D. Gautier, J. A. Haberman, D. N. Harpold, W. T. Kasprzak, J. I. Lunine, T. C. Owen, and F. Raulin (2010), Composition of Titan's lower atmosphere and simple surface volatiles as measured by the Cassini-Huygens probe gas chromatograph

- mass spectrometer experiment, *J. Geophys. Res.*, *115*, E12006, doi:10.1029/2010JE003659.
- Perron, J. T., M. P. Lamb, C. D. Koven, I. Y. Fung, E. Yager, and M. Ádámkóvics (2006), Valley formation and methane precipitation rates on Titan, *J. Geophys. Res.*, *111*, E11001, doi:10.1029/2005JE002602.
- Schneider, T., S. D. B. Graves, E. L. Schaller, and M. E. Brown (2012), Polar methane accumulation and rainstorms on Titan from simulations of the methane cycle, *Nature*, *481*, 58–61.
- Stofan, E. R., et al. (2007), The lakes of Titan, *Nature*, *445*, 61–64.
- Tomasko, M. G., et al. (2005), Rain, winds and haze during the Huygens probe's descent to Titan's surface, *Nature*, *438*, 765–778.
- Turtle, E. P., et al. (2011), Rapid and extensive surface changes near Titan's equator: Evidence of April showers, *Science*, *331*, 1414–1417.
- Wasiak, F. C., A. Luspáy-Kuti, W. Welivitiya, L. Roe, V. F. Chevrier, D. G. Blackburn, and T. Cornet (2012), A facility for simulating Titan's environment, *Adv. Space Res.*, doi:10.1016/j.asr.2012.10.020, in press.
- Williams, K. E., C. P. McKay, and F. Persson (2012), The surface energy balance at the Huygens landing site and the moist surface conditions on Titan, *Planet. Space Sci.*, *60*, 376–385.